JOURNAL OF APPLIED ELECTROCHEMISTRY 25 (1995) 315–325

Discharge behaviour of tubular lead dioxide electrodes Part III: Two-dimensional current density distribution

J. LANDFORS*, D. SIMONSSON

Department of Chemical Engineering, Division of Applied Electrochemistry, The Royal Institute of Technology, S-100 44 Stockholm, Sweden

R. E. WHITE

Department of Chemical Engineering, University of South Carolina, Columbia SC 29208, USA

Received 17 March 1994; revised 17 August 1994

The initial current density distribution in lead acid batteries with tubular lead dioxide electrodes and flat lead electrodes has been studied by means of a two-dimensional model and experimental verification by polarization curves and potential transients during galvanostatic discharge. The cell geometry was modelled with and without separators and a tubular electrode envelope. The governing equations were solved with a finite element method. It was found that the tube envelope has a large impact on the current density distribution and had to be incorporated into the model to fit the experimental results. Although the envelope increases the ohmic losses, it has the positive effect of giving a more uniform current distribution around the electrode tube. A lead acid cell with tubular positive electrodes and flat negative electrodes can therefore be approximated by a one-dimensional model consisting of a positive electrode tube placed concentrically in a cylindrical lead electrode. The two-dimensional model was further used to study the effects of different design factors, for example, cell width and kinetic parameters of the lead dioxide electrode.

List of symbols

d	half thickness of the lead electrode (m)
E	electrode potential (V)
E_a^{Rev}	equilibrium potential of the lead electrode vs NHE (V)
E_c^{Rev}	equilibrium potential of the lead dioxide electrode vs NHE (V)
F	Faraday constant (96 487 A s mol^{-1})
i_2	current density in the solution phase (A m^{-2})
I	total cell current (A m^{-1})
j	local current true current density per unit volume of electrode (A m^{-3})
j_0	apparent exchange current density (A m^{-2})
$\bar{j}$	normalized local current density
L	length of the unit cell (m)
r_0	radius of current collector in the positive electrode (m)
R	outer radius of active material of the positive electrode (m)
$\mathscr{R}$	universal gas constant (8.3143 J mol^{-1} K^{-1})
S	specific surface area (m^{-1})
s	thickness of the microporous separator (m)
T	absolute temperature (K)
ΔU	difference between open circuit voltage and cell voltage during discharge (V)

Greek symbols

δ	thickness of the positive electrode envelope, (m)
ϵ	porosity
η	overvoltage (V)
κ	conductivity (Ω^{-1} m^{-1})
κ_{eff}	effective conductivity (Ω^{-1} m^{-1})
ϕ	potential (V)
ω	width of unit cell (m)
θ	angle in the cross section of the positive electrode tube

Subscripts

1	solid phase
2	solution phase
I–VI	regions in the unit cell (see Fig. 2)
a	anode
c	cathode
av	average

1. Introduction

Lead–acid batteries with tubular lead dioxide electrodes are primarily used in applications with high requirements on service life and reliability. High cycle life is an important feature for tractionary applications. However, the comparably low energy density often limits the use to electrical trucks and other heavy-weight vehicles. It is, therefore, of interest to increase the understanding of how electrochemical engineering

* *Present address*: Eka Nobel, Electrochemicals Division, R&D Department, Box 13000, S-850 13 Sundsvall, Sweden

0021-891X © 1995 Chapman & Hall

can be used to improve the behaviour of tubular lead dioxide electrodes with a focus on increasing the energy density while retaining long cycle life.

The understanding of lead–acid batteries with flat pasted electrodes has been greatly increased over the last two decades by application of theories for porous electrodes. Models for prediction of the discharge behaviour have been developed for separate electrodes [1–6] as well as for complete cells [7, 8]. Although a large number of scientific papers have been presented over the years, there are relatively few publications related to models for the special geometry in cells with tubular electrodes. Most investigations are empirical and very few use theories for current density distribution and mass transport in porous electrodes. A one-dimensional discharge model has been presented by Lin *et al.* [9]. It was based on a pseudo steady-state approach with an infinitely thin current collector in the centre of the electrode. Their results, valid in the low current density range, indicated that the formation of lead sulphate during discharge starts from the interior part of the positive electrode.

However, their results have later been contradicted by experimental [10] and theoretical [11] results. A time dependent discharge model was developed in order to take into consideration the radius of the current collector rod, the tube envelope, and an extended current density range. It was found that the electrode behaviour during discharge could be fairly well described by a one-dimensional model and that the formation of lead sulphate starts from the exterior part of the electrode tubes. The results were also experimentally verified by polarization measurements, discharge capacity tests, and sulphur distributions over the cross sections of the electrodes. It was also concluded that the tube envelope, which was not considered in the model by Lin *et al.*, has a very large impact on the migration and diffusion properties of the electrode and has to be considered as time dependent in the model to fit experimental data.

Mao, White and Jay [7] studied the initial two-dimensional current distribution in a lead–acid cell with tubular current collectors but with flat electrodes. Their results indicated that there were no large differences in the local current density over the other surface of the electrodes.

A schematic of a lead–acid cell with tubular lead dioxide electrodes is shown in Fig. 1. It can be seen that the geometry, if neglecting the cell height, has to be regarded as two-dimensional to describe the current and potential distribution. The two-dimensional current distribution in this system has previously been studied by Euler and Horn [12]. They used an analogue electric circuit as a model and concluded that the current density distribution was fairly uniform at low current densities. However, at higher current densities, the polarization does not increase linearly with the current density and the discharge reaction is governed by Tafel kinetics. Consequently, it can be assumed that the current distribution is more nonuniform at high current densities than what could be predicted by the model of Euler and Horn.

Therefore, the aim of this paper is to present the derivation and application of a model for the initial current density distribution in a lead–acid cell with tubular lead dioxide electrodes comprising two-dimensional geometry, experimentally verified kinetic parameters, a separator region, and a tube envelope. The aim is also to determine if the one-dimensional time dependent model derived earlier [11] has to be extended to two dimensions to improve the possibility to predict and optimize the cell.

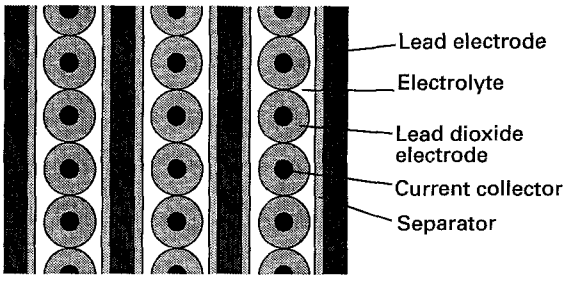

Fig. 1. Electrode assembly with tubular lead dioxide electrodes, view from above.

2. Experimental details

The experimental procedures have been described elsewhere [10]. This paper deals only with the plane-cylindrical geometry comprising tubular lead dioxide electrodes and flat pasted lead electrodes with a cell height of 135 mm. The experimental cell consisted of three positive electrode tubes symmetrically placed between two flat pasted lead electrodes. The polarization of the lead dioxide electrodes was measured relative to a Hg/Hg_2SO_4 reference electrode in saturated solution of K_2SO_4. The measuring points were located at the middle of the cell height at two different positions ($x = 0$, $y = R + \delta$) and ($x = \omega$, $y = 0$)

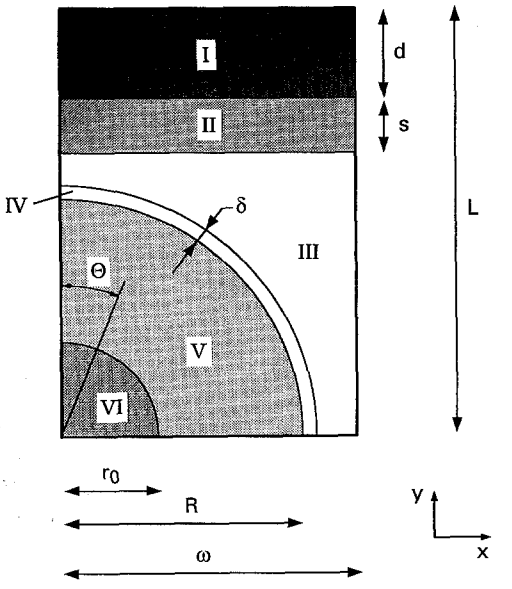

Fig. 2. Unit cell.

as shown in Fig. 2. ($x = 0$, $y = 0$) is located in the centre of the current collector in the tubular electrode. The overpotentials are given relative to the rest potential of the electrodes in the electrolyte.

3. Mathematical model

3.1. *Basic assumptions*

The unit cell, Fig. 2, consists of six different regions referred to by the Roman numerals I to VI and with the following definitions:

(I) Porous lead electrode with half the thickness of a full size plate.
(II) Microporous separator.
(III) Free electrolyte.
(IV) Tube envelope zone.
(V) One quarter of the cross section of a porous lead dioxide tube electrode.
(VI) One quarter of the cross section of the current collector spine in the positive electrode.

Fig. 2 also gives the definitions of the geometrical parameters of the cell. The problem is further simplified by introduction of the following assumptions:

(i) The conductivities of the lead current collectors in both the lead and the lead dioxide electrodes are high enough not to cause any significant effect on the vertical potential drop in the cell [13]. The model can thus be restricted to two dimensions.
(ii) The electrical conductivities of the porous lead and lead dioxide, region I and V, respectively, are high compared with the pore solution conductivity.
(iii) The lead dioxide enclosed in the pores of the envelope, region III, has been fully discharged to lead sulphate. It has been experimentally verified [10] that this takes place during the initial period of the discharge. Region III can therefore be regarded as a porous inactive separator.
(iv) The lead grid in region VI is a macrohomogeneous part of the porous lead electrode.
(v) All porous regions, I to V, are isotropic and filled with sulphuric acid of uniform concentration.

3.2. *Model equations*

3.2.1. The lead electrode, region I. The current density distribution in region I is governed by the current balance

$$\nabla \cdot \vec{i}_{2,\mathrm{I}} = j_{\mathrm{I}} \tag{1}$$

The expression for the electrode kinetics [6] is

$$j_{\mathrm{I}} = \frac{S_{\mathrm{I}} j_{0,\mathrm{I}} \left[1 - \exp\left(\frac{2F}{\mathscr{R}T}\eta_{\mathrm{a}}\right)\right]}{S_{\mathrm{I}} j_{0,\mathrm{I}}/j_{\mathrm{lim}} - \exp\left(\frac{\alpha_{\mathrm{c,I}} F}{\mathscr{R}T}\eta_{\mathrm{a}}\right)} \tag{2}$$

where

$$\eta_{\mathrm{I}} = \phi_{1,\mathrm{I}} - \phi_2 - E_{\mathrm{a}}^{\mathrm{Rev}} \tag{3}$$

and Ohm's law in the electrolyte phase

$$\vec{i}_{2,I} = -\kappa_{\mathrm{eff,I}} \nabla \phi_2 \tag{4}$$

Equations 1 to 4 are then subject to the following boundary conditions:

$$\left.\begin{aligned} \vec{i}_{2,\mathrm{I}} &= 0 \\ \nabla\phi_2 &= 0 \end{aligned}\right\} \quad \text{at } y = L \tag{5,6}$$

$$\frac{\partial \phi_2}{\partial x} = 0 \quad \text{at } x = 0 \text{ for } L - d < y < L \tag{7}$$

$$\frac{\partial \phi_2}{\partial x} = 0 \quad \text{at } x = \omega \text{ for } L - d < y < L \tag{8}$$

and

$$\kappa_{\mathrm{eff,I}} \nabla \phi_{2,\mathrm{I}} = \kappa_{\mathrm{eff,II}} \nabla \phi_{2,\mathrm{II}} \tag{9}$$

3.2.2. The lead dioxide electrode, region V. The current density distribution in the positive electrode is governed by the same general equations as the negative electrode in the following way:

Current balance

$$\nabla \cdot \vec{i}_{2,\mathrm{V}} = j_{\mathrm{V}} \tag{10}$$

The electrode kinetics [1]

$$j_{\mathrm{V}} = S_{\mathrm{V}} j_{0,\mathrm{V}} \left[\exp\left(\frac{(2 - \alpha_{\mathrm{c,V}})F}{\mathscr{R}T}\eta_{\mathrm{c}}\right) - \exp\left(\frac{\alpha_{\mathrm{c,V}} F}{\mathscr{R}T}\eta_{\mathrm{c}}\right)\right] \tag{11}$$

with

$$\eta_{\mathrm{V}} = \phi_{1,\mathrm{V}} - \phi_2 - E_{\mathrm{c}}^{\mathrm{Rev}} \tag{12}$$

and Ohms' law in the electrolyte phase

$$\vec{i}_{2,\mathrm{V}} = -\kappa_{\mathrm{eff,V}} \nabla \phi_2 \tag{13}$$

The boundary conditions for region V become

$$\left.\begin{aligned} \vec{i}_{2,\mathrm{V}} &= 0 \\ \nabla\phi_{2,\mathrm{V}} &= 0 \\ \phi_{1,\mathrm{V}} &= 0 \end{aligned}\right\} \quad \text{at } x^2 + y^2 = r_0^2 \tag{14,15,16}$$

$$\frac{\partial \phi_2}{\partial y} = 0 \quad \text{at } y = 0 \text{ for } r_0 < x < R \tag{17}$$

$$\frac{\partial \phi_2}{\partial x} = 0 \quad \text{at } x = 0 \text{ for } r_0 < x < R \tag{18}$$

and

$$\kappa_{\mathrm{eff,V}} \nabla \phi_{2,\mathrm{V}} = \kappa_{\mathrm{eff,IV}} \nabla \phi_{2,\mathrm{IV}} \quad \text{at } x^2 + y^2 = R^2 \tag{19}$$

3.2.3. Separator, free electrolyte and tube envelope, regions II, III, and IV. The regions between the anode and the cathode are governed by the Laplace equation

$$\nabla^2 \phi_2 = 0 \tag{20}$$

with the boundary conditions

$$\frac{\partial \phi_2}{\partial x} = 0 \quad \text{at } x = 0 \text{ for } R < y < L - d \tag{21}$$

$$\frac{\partial \phi_2}{\partial y} = 0 \quad \text{at } x = \omega \text{ for } 0 < y < L - d \tag{22}$$

$$\frac{\partial \phi_2}{\partial y} = 0 \quad \text{at } y = 0 \text{ for } R < x < \omega \tag{23}$$

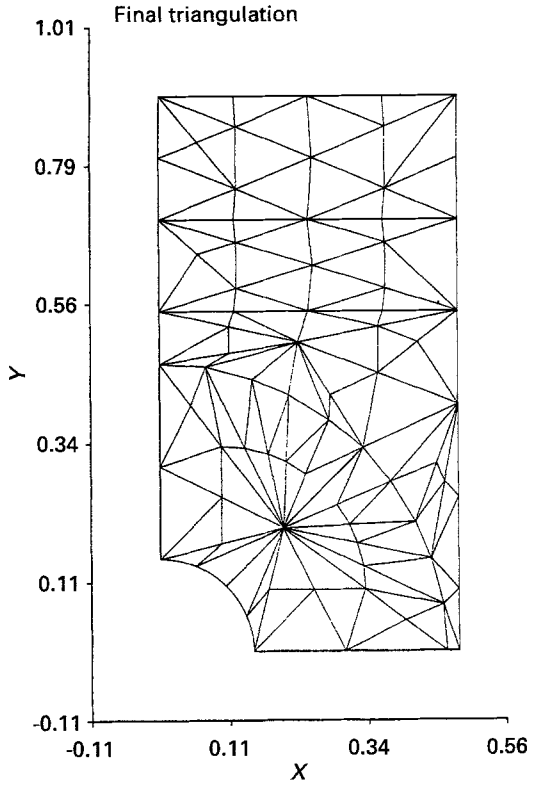

Fig. 3. Final triangulation of a unit cell without envelope and separator.

and

$$\kappa_{\text{eff,II}}\nabla\phi_{2,\text{II}} = \kappa_{\text{eff,III}}\nabla\phi_{2,\text{III}} \quad (24)$$

$$\kappa_{\text{eff,III}}\nabla\phi_{2,\text{III}} = \kappa_{\text{eff,IV}}\nabla\phi_{2,\text{IV}} \quad (25)$$

for the interface between region III and IV.

3.3. *Numerical solution*

The system of equations was solved with a finite element technique provided in the PDE/PROTRAN program package by IMSL, Incorporated [14]. The domain was initially divided into a few triangles defined by the positions of their corners. The triangular network was then automatically refined during the computation to obtain sufficient accuracy over the unit cell region.

Curved outer boundaries (i.e., the current collector), can be relatively easily treated with the PDE/PROTRAN package by defining an analytical expression. However, a curved internal boundary cannot be defined by an equation. Therefore, the interface between region IV and V was approximated by 10 straight lines of equal length. The interface between region III and IV was treated in a similar way. The final triangulation for a simplified case without separator and tube envelope is shown in Fig. 3.

4. Results

The current density distribution in a cell with tubular lead dioxide electrodes and flat pasted negative electrodes was analysed with respect to geometrical dimensions, separators and kinetic parameters. Two different cases were studied: (i) a cell without separator and tube envelope around the positive tube and (ii) a cell with tube envelope and a microporous separator closest to the lead electrode. Some calculations were also done on a cell with tube envelope but without the separator. The numerical values used in the calculations are given in Table 1, unless otherwise stated. The calculations were performed at a given deviation, ΔU, from the open circuit voltage, V_{ocv}, defined as

$$\Delta U = V_{\text{ocv}} - (E_{\text{a}} - E_{\text{c}}) \quad (26)$$

Table 1. Values of parameters used in the model in the standard case

Parameter	*Value*	*Ref.*
d	2.00×10^{-3} m	
L	9.00×10^{-3} m	
R	4.45×10^{-3} m with envelope	
	4.65×10^{-3} m without envelope	
r_0	1.50×10^{-3} m	
s	1.50×10^{-3} m	
ω	5.00×10^{-3} m	
δ	0.25×10^{-3} m	
ϵ_{II}	0.65	
ϵ_{IV}	0.09	
κ^0	$78.8\,\Omega^{-1}\,\text{m}^{-1}$	8
Lead electrode, region I		
$\kappa_{\text{eff,I}}$	$23\,\Omega^{-1}\,\text{m}^{-1}$	6
$S_{\text{I}}\,j_{0,\text{I}}$	$1.9 \times 10^{5}\,\text{A m}^{-3}$	6
j_{lim}	$-1 \times 10^{5}\,\text{A m}^{-3}$	6
$\alpha_{\text{c,I}}$	0.9	6
Lead dioxide electrode, region V		
$\kappa_{\text{eff,V}}$	$22\,\Omega^{-1}\,\text{m}^{-1}$	10
$S_{\text{V}}\,j_{0,\text{V}}$	$1862\,\text{A m}^{-3}$	10
$\alpha_{\text{c,V}}$	2	10

4.1. *Cell without envelope and separator*

The results from the simplified model with only free

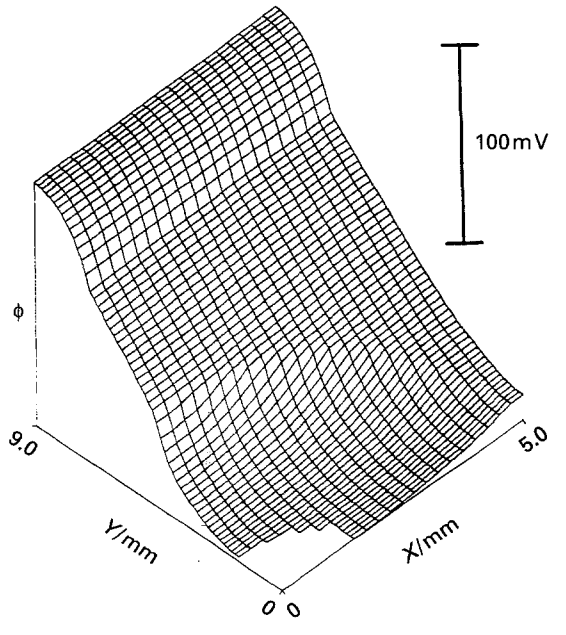

Fig. 4. Predicted potential distribution in a cell without envelope and separator at $\Delta U = 0.2$ V.

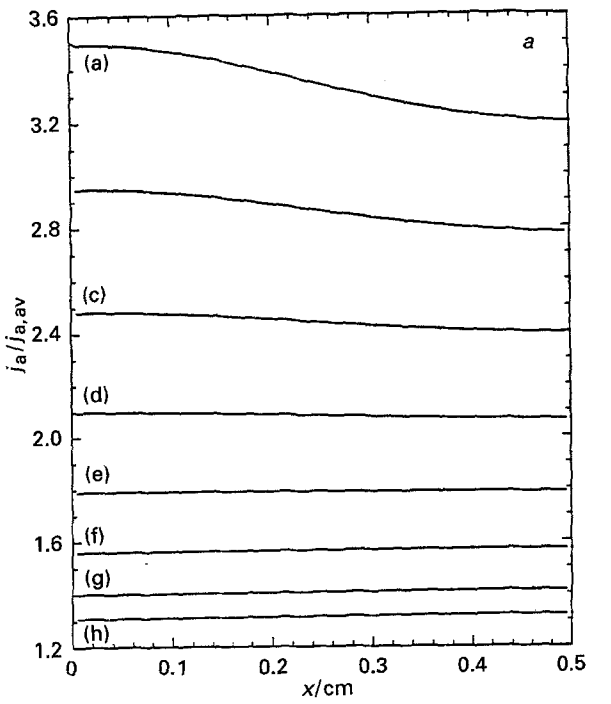

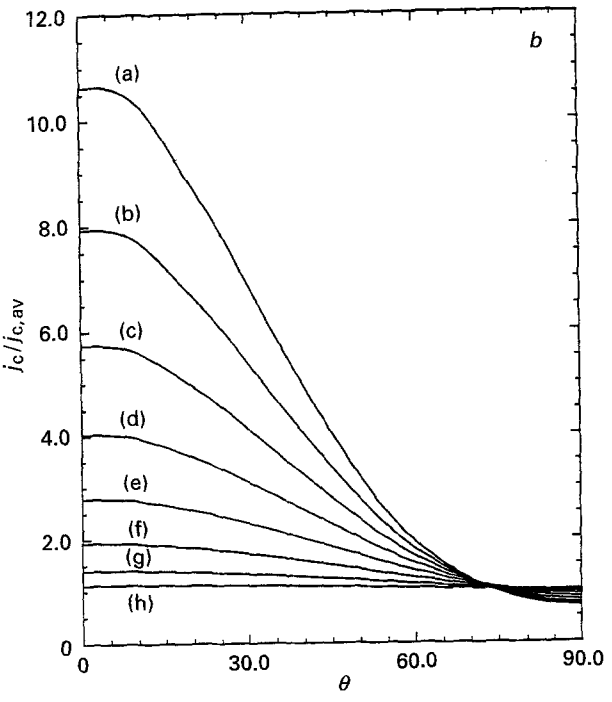

Fig. 5. Normalized current density distribution along the outer surface of (*a*) the lead and (*b*) the lead dioxide electrode. Both Figures *a* and *b*, respectively, have ΔU equal to (a) 0.2, (b) 0.175, (c) 0.15, (d) 0.125, (e) 0.1, (f) 0.075, (g) 0.05 and (h) 0.025 V. Cell without envelope or separator.

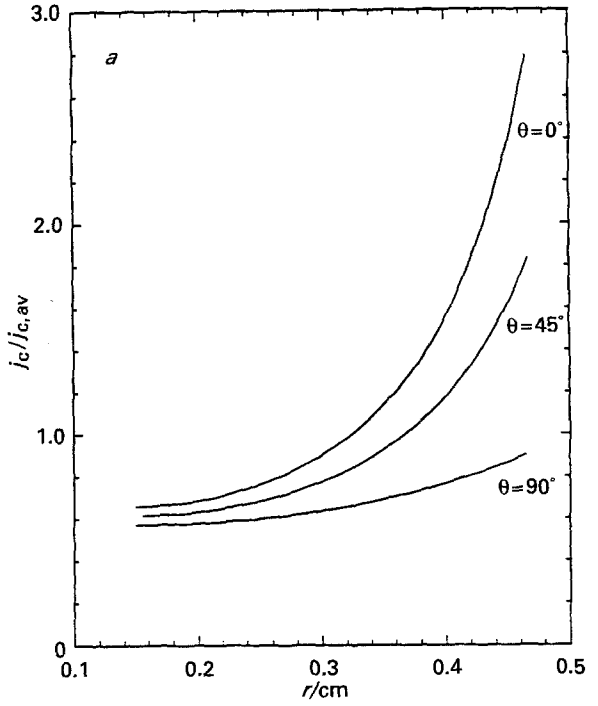

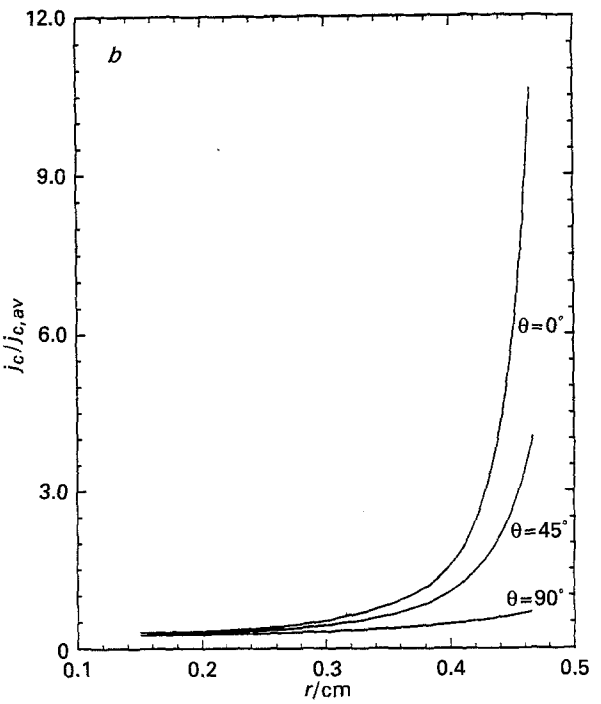

Fig. 6. Normalized current density along different cross sections of a tubular electrode without envelope (*a*) at $\Delta U = 0.1$ V and (*b*) at $\Delta U = 0.2$ V.

sulphuric acid between the electrodes are shown in Figs 4 to 6. The three dimensional plot of the potential distribution at $\Delta U = 0.2$ V, Fig. 4, shows that the potential in the lead electrode varies mainly in the y-direction, while there are no significant variations along the outer surface of the electrode. The behaviour is very similar for what is seen in the cells with plane parallel plates and consequently it can be concluded that the negative electrode in cells with tubular positives could be fairly well described by a one-dimensional approach. It is further reasonable to assume that the lead electrode will behave as a one-dimensional flat pasted electrode, for which there are well-developed time-dependent models, also during discharge.

The tubular electrode, on the other hand, shows large variation in the potential distribution both in the x and y-directions. The overpotential varies significantly over the outer surface of the electrode tube with a maximum at the point closest to the negative electrode and a minimum at $y = 0$. It can therefore be concluded that the tubular electrode in this case has to be treated as truly two-dimensional and has to be so also for time-dependent discharge models.

To compare the relative utilization over the cross sections of the electrodes, a normalized local current density for the negative electrode was defined as

$$\bar{j}_{\mathrm{I}} = \frac{j_{\mathrm{I}}}{j_{\mathrm{I,av}}} \tag{27}$$

and for the positive electrode

$$\bar{j}_{\mathrm{V}} = \frac{j_{\mathrm{V}}}{j_{\mathrm{V,av}}} \tag{28}$$

The average true local current densities, $j_{\mathrm{I,av}}$ and $j_{\mathrm{V,av}}$, were calculated by dividing the total cell current, I, with the cross sectional area of the anode and the cathode, respectively. The total cell current was calculated by integrating the local current density over the cross section of the lead electrode according to the equation

$$I = \int_{L-d}^{L} \int_{0}^{\omega} j_{\mathrm{I}} \, \mathrm{d}x \, \mathrm{d}y \tag{29}$$

Normalized current densities along the outer surface of the lead and the lead dioxide electrode are shown in Fig. 5(a) and (b), respectively, for different values of ΔU. As can be seen in Fig. 5(a), the current distribution does not vary significantly over the outer surface of the lead electrode. It is only at very high current densities, $1219\,\mathrm{A\,m^{-2}}$ ($\Delta U = 0.2\,\mathrm{V}$), that there is a slightly higher discharge rate of about 10% in the parts of the electrodes closest to the positive tube. The relatively low values of the normalized current densities also indicate that the utilization of the lead electrode in the thickness of the lead electrode is fairly uniform. However, in the tubular positive electrode, the normalized current densities show large variations over the tube surface, see Fig. 5(b). This confirms the results discussed in connection with the potential distribution. At $1219\,\mathrm{A\,m^{-2}}$, the normalized current density exceeds 10 in the parts closest to the lead electrode while it is lower than 1 at $\theta = 90°$. It is also clear that there is a large variation in the discharge rate over the cross section of the electrode and that the effect of increasing current density is highest in the parts closest to the lead electrode, which could be expected from the fundamental rules of current distribution. Also, there seems to be a point in the positive electrode at about $\theta = 75°$ where the normalized current density is equal to unity, irrespective of the value of ΔU.

The current density distribution inside the tubular lead dioxide electrode is illustrated in another way in Fig. 6(a) and (b), which show the normalized current density as a function of the radius, r, along different angular directions at two different values of ΔU, 0.1 and 0.2 V. Also in this case it is clearly seen that the outer parts of the electrode tube are exposed to an extremely high current density during the initial period of the discharge.

4.2. *Cell with tube envelope and separator*

The separator was included in the model by adding a domain, region II in Fig. 2, with a decreased conductivity in direct contact with the lead electrode. The effective conductivity of the separator was assumed to depend on the porosity according to the equation

$$\kappa_{\mathrm{eff,II}} = \kappa^{0} \epsilon_{\mathrm{II}}^{1.5} \tag{30}$$

In earlier work [1, 2] it was found that the lead dioxide enclosed in the envelope region plays an important role for the discharge behaviour of tubular electrodes. The formation of lead sulphate in the pores of the envelope affects migration and diffusion and thus increases the potential losses and decreases the rate of diffusion of sulphuric acid from the free electrolyte into the porous structure. However, the total amount of lead dioxide in the envelope is small and does not contribute significantly to the total discharge capacity. It was also found that lead dioxide in the envelope zone is reduced in the very beginning of the discharge and forms a more or less time independent porous layer. The tube envelope was therefore assumed to be macrohomogeneous and the lead dioxide in the pores of the envelope was fully discharged and converted to $PbSO_4$. Thus, the region could be implemented into the model as an inactive separator around the tube and the effective conductivity over the zone calculated by Equation 30.

Comparison of Figs 4 and 7 shows that the potential distribution is strongly affected by the introduction of the envelope. A distinct voltage drop appears around the positive electrode. The effect of the separator is small compared to the envelope and can be seen as a slight discontinuity in the electrolyte region in Fig. 7. It is also notable that the potential differences over the cross section of the lead dioxide electrode are smaller when compared to the case without a tube envelope,

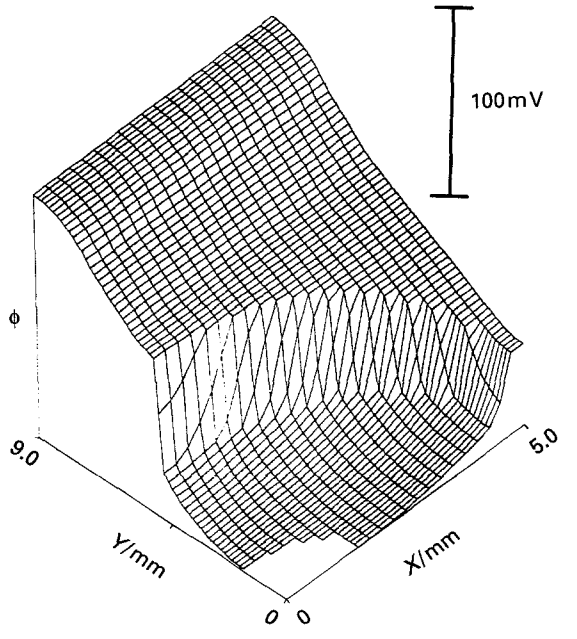

Fig. 7. Predicted potential distribution in a cell with envelope and separator at $\Delta U = 0.2\,\mathrm{V}$.

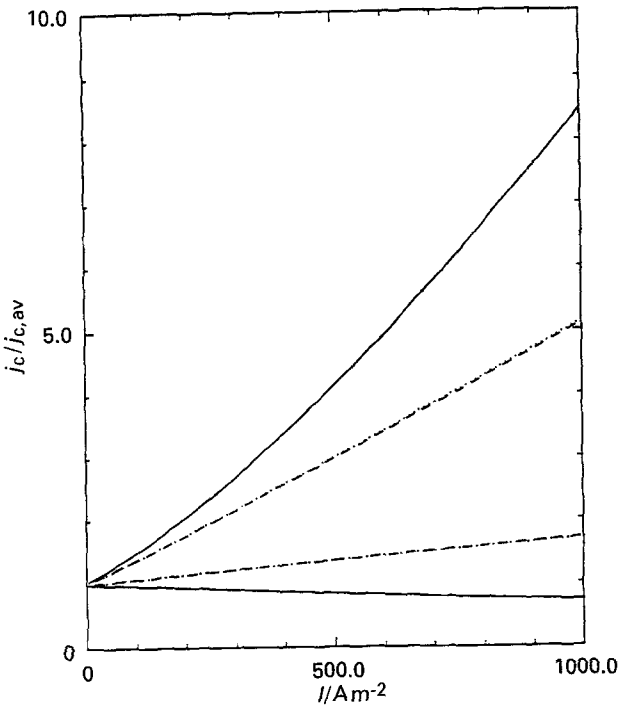

Fig. 8. Normalized current densities as functions of the geometrical current density at ($x = R$, $y = 0$), lower lines, and ($x = 0$, $y = R$), upper lines, for three different cases: (i) cell without envelope and separator (solid lines); (ii) cell with envelope but without separator (dashed lines) and (iii) cell with envelope and separator (dotted lines).

Fig. 4. In the lead electrode there does not seem to be very large differences compared with the first case.

To compare the discharge rate in different regions of the lead dioxide electrodes, the normalized current densities in two positions, ($x = R$, $y = 0$) lower lines and ($x = 0$, $y = R$) upper lines, have been plotted against the geometrical current density for three different cases, Fig. 8:

(i) without envelope and separator (solid lines)
(ii) with envelope but without separator (dashed lines)
(iii) with envelope and separator (dotted lines).

For case (i) it can be seen that the normalized current density increases with increasing geometrical current density at ($x = 0$, $y = R$) while it decreases at ($x = R$, $y = 0$). This is also the worst case with respect to current distribution. A cell with a tubular electrode envelope, case (ii), has a more uniform distribution in the positive electrode. The normalized current density increases with increasing geometrical current density at both ($x = 0$, $y = R$) and ($x = R$, $y = 0$). Fig. 8 also shows the behaviour of a cell with both an envelope and a separator. It can once again be clearly seen that the microporous separator has a negligible effect on the current distribution compared with the tube envelope.

Although the tube envelope has a positive effect on the current density distribution and acts as an equalizer of the current around the electrode tube, it gives a significant increase in the overall cell resistance. This can be clearly seen in Fig. 9 that shows polarization curves for cases (i) (solid line), (ii) (dashed line) and (iii) (dotted line). At a geometrical current density of

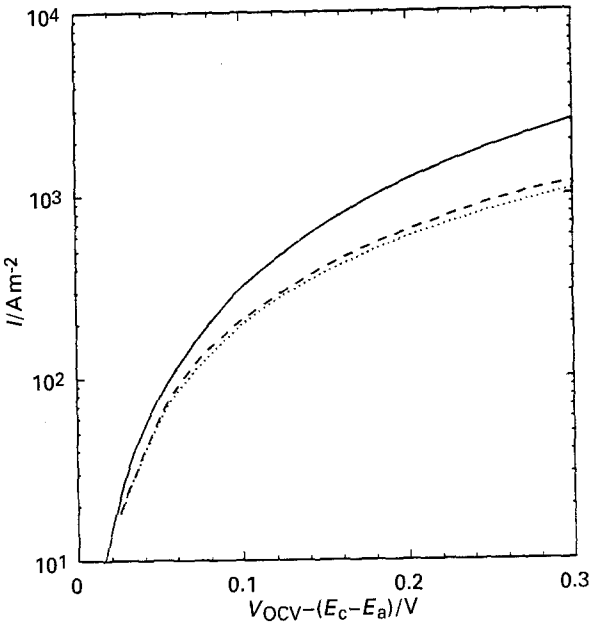

Fig. 9. Polarization curves for three different cell configurations: (i) cell without envelope and separator (solid lines); (ii) cell with envelope but without separator (dashed lines) and (iii) cell with envelope and separator (dotted lines).

$1000\,A\,m^{-2}$, the increase in the potential drop is about 80 mV due to the envelope and about 15–20 mV due to the separator.

5. Model validation

In the following Section, the qualitative and quantitative validity of the model will be discussed. For this purpose, experimentally obtained polarization curves and galvanostatic discharge curves will be compared with the model output. The measurements were performed in a cell without microporous separator but with an envelope around the positive electrode tube. Luggin capillaries were placed at ($x = \omega$, $y = 0$) and at ($x = 0$, $y = 0.47$ cm).

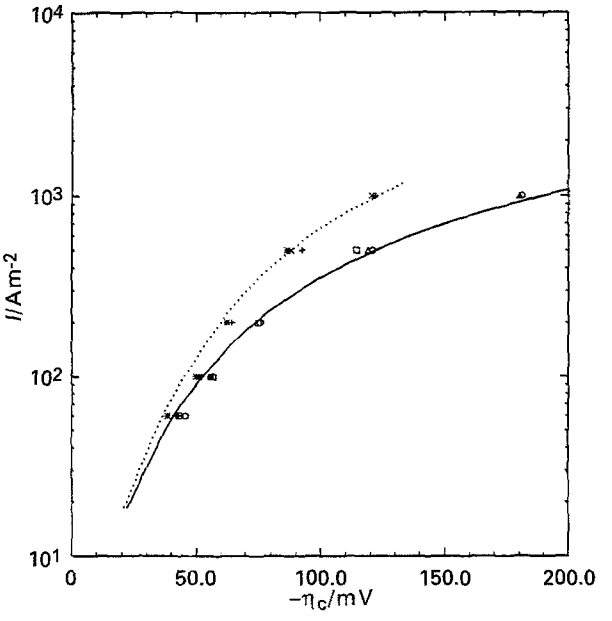

Fig. 10. Calculated polarization curves and experimental data (symbols) at ($x = 0$, $y = 0.47$ cm) (solid line) and at ($x = \omega$, $y = 0$) (dotted line).

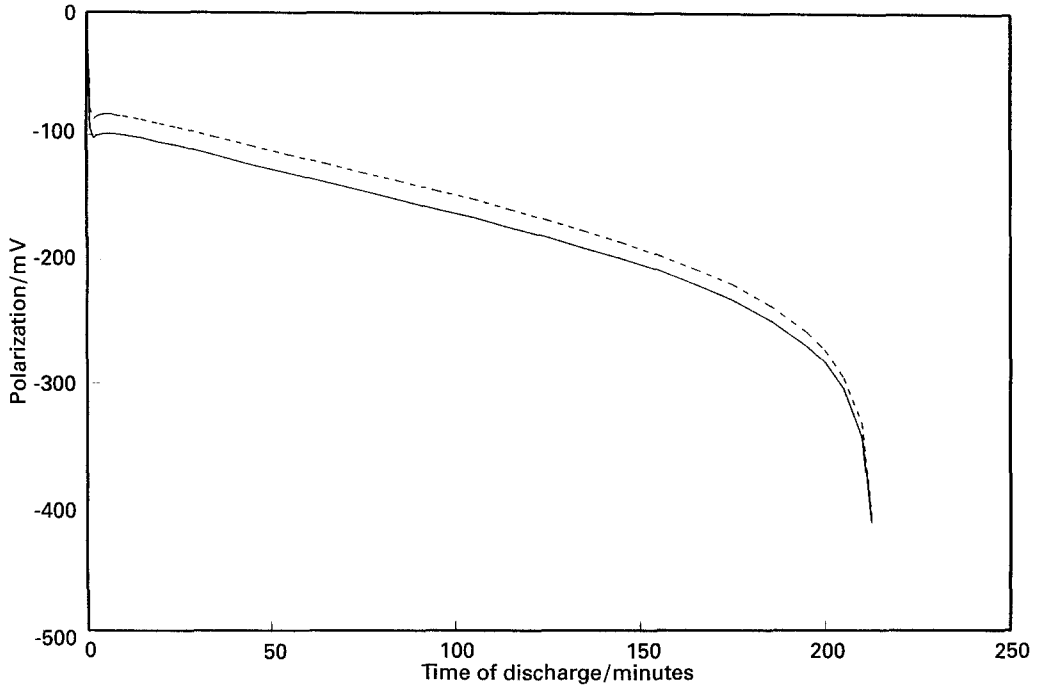

Fig. 11. Overpotentials at ($x = 0$, $y = 0.47$ cm) (solid line) and at ($x = \omega$, $y = 0$) (dotted line) as a function of time during galvanostatic discharge at a geometrical current density of 200 A m^{-2}.

5.1. *Polarization curves*

Figure 10 shows calculated polarization curves at the measuring points, solid line ($x = 0$, $y = 0.47$ cm) and dotted line ($x = \omega$, $y = 0$). The geometrical current density in the cell is plotted as a function of the cathodic overpotential during discharge. Experimental data are from measurements on two separate electrodes with unfilled symbols at ($x = 0$, $y = 0.47$ cm) and the other symbols at ($x = \omega$, $y = 0$). It can be seen that the model can be used to predict the polarization behaviour with an accuracy of about 5 mV in a current density range from about 60 to 1000 A m^{-2}. However, it must be stressed that the polarization is governed to a large extent by the envelope resistance. Since the amount of lead dioxide in the envelope zone can vary from one electrode tube to the other, there can be large variations in the polarization behaviour and consequently also in the accuracy of the model prediction. Nevertheless, the polarization measurements verify the assumptions made in the model and support the conclusion that the *iR*-drop over the envelope zone is significant and that it has a positive effect on the current density distribution in the positive electrode.

Table 2. Comparison of measured and predicted potential differences between two measuring points in a cell during galvanostatic discharge

Current density /A m^{-2}	*Measured potential difference*/mV	*Calculated potential difference*/mV
200	15	14
1000	56	65

5.2. *Galvanostatic discharge*

Cells were galvanostatically discharged at 200 and 1000 A m^{-2}, see Figs 11 and 12, respectively. The potentials were measured at the same positions as for the polarization measurements. It can be seen that the discharge starts with the characteristic voltage dip in both measuring points. Fairly soon, a difference in the polarization between the measuring points is established and maintained during the major part of the discharge. A comparison of Figs 11 and 12 with Fig. 10 shows that the polarization differences in different parts of the cell during galvanostatic discharge can be fairly well estimated by the model. A comparison between experimentally obtained and the calculated potential difference between the capillaries is given in Table 2. It can be seen that the accuracy is about 20%. It must however be emphasised that a direct comparison between the measured potential differences during galvanostatic discharge and the calculated values is not fully accurate since the polarization curves in Fig. 10 were made by intermittent discharge of electrodes that initially had been discharged to about 7% of the rated discharge capacity to avoid the effects of the initial potential dip. The galvanostatic discharge can, therefore, give a different behaviour of the envelope zone than what was expected from the model. Also, the model gives the values at a constant initial concentration while large concentration gradients are developed during the discharge process.

6. Discussion

The model has also been used to study the effects of some design parameters that could be of relevance

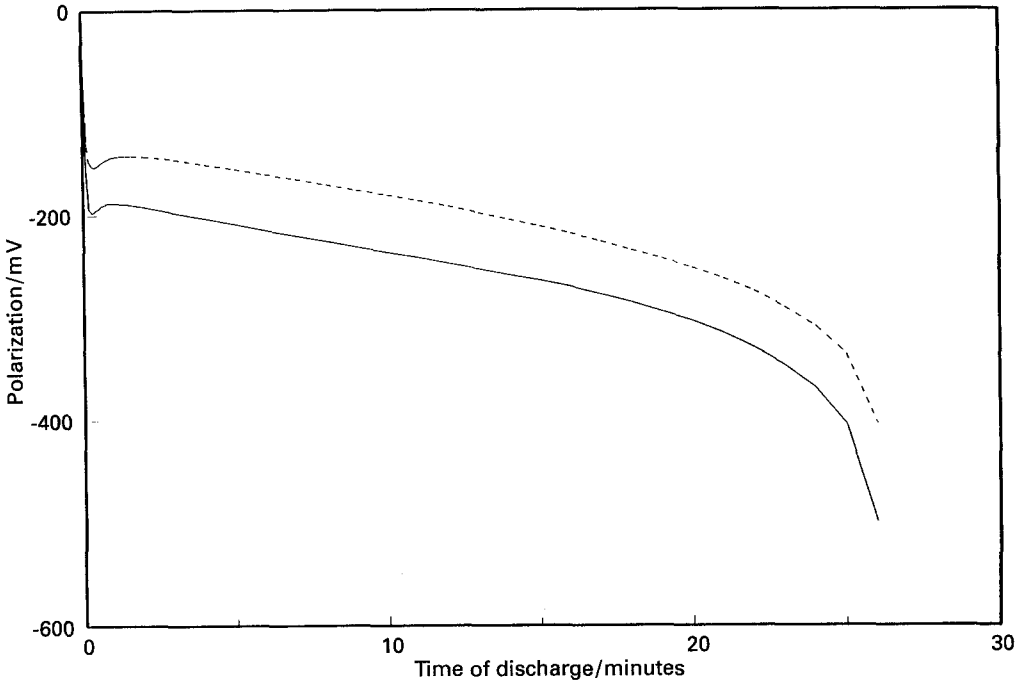

Fig. 12. Overpotentials at ($x = 0$, $y = 0.47$ cm) (solid line) and at ($x = \omega$, $y = 0$) (dotted line) as a function of time during galvanostatic discharge at a geometrical current density of 1000 A m^{-2}.

to the cell performance. Figure 13 shows how the normalized local current densities at the outer surface of the positive electrode at ($x = 0$, $y = R$) and ($x = R$, $y = 0$) vary with the geometric current density at different values of the cell width, ω. It can be seen that it is possible to improve the current distribution by increasing the width of the unit cell and maintaining the radius of the electrode tube, that is, by increasing the gap between each individual tube. However, the effect is fairly small even at $\omega = 7$ mm, which corresponds to gap of 2.18 mm for tubes with envelope. It is doubtful if such an improvement is justified in comparison to the increased battery volume.

The effects of changing the electrochemically active surface area of the positive electrode in a cell without envelope or separator are shown in Figs 14 and 15. For three different values of $Sj_{0,V}$, 5000, 1862, and 500 A m^{-3}, it can be seen that the current

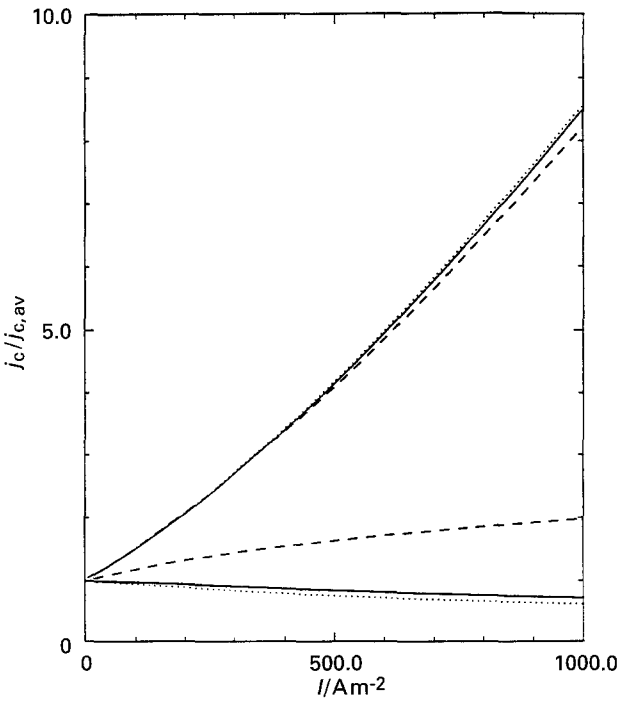

Fig. 13. Normalized local current densities as functions of geometrical current density in a cell without envelope and separator at ($x = R$, $y = 0$), lower lines, and ($x = 0$, $y = R$), upper lines, at $\omega = 0.485$ cm (dotted lines), $\omega = 0.5$ cm (solid lines), and $\omega = 0.7$ cm (dashed lines).

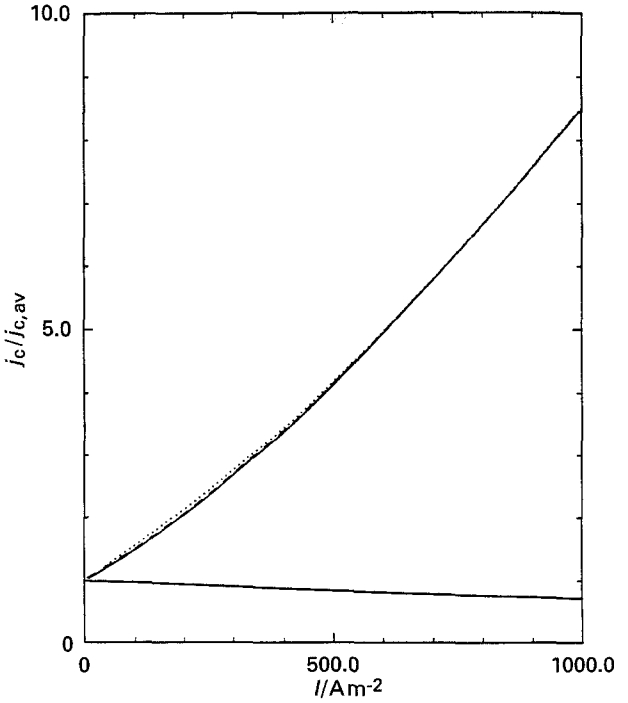

Fig. 14. Normalized local current densities as functions of geometrical current density in a cell without envelope and separator at ($x = R$, $y = 0$), lower lines, and ($x = 0$, $y = R$), upper lines, with $S_{j0,V} = 5 \times 10^{-3}$ (dashed lines), 1.862×10^{-3} (solid lines) and 5×10^{-4} A cm^{-3} (dotted lines).

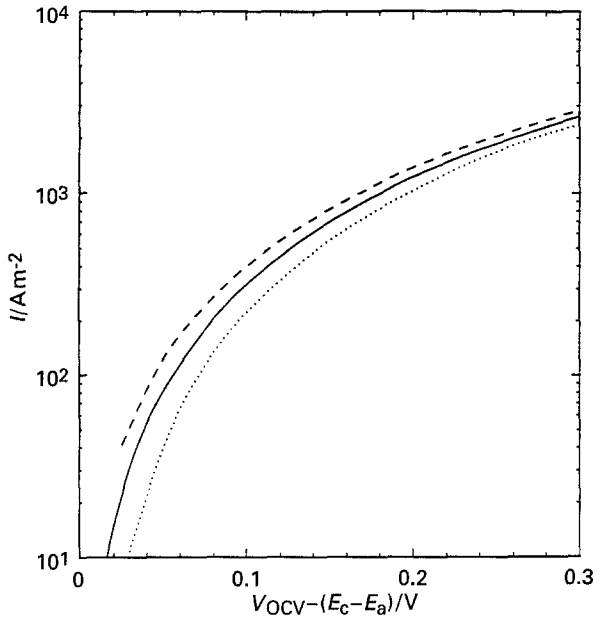

Fig. 15. Geometrical current densities as functions of ΔU for a cell without envelope and separator with $S_{j0,V} = 5 \times 10^{-3}$ (dashed line), 1.862×10^{-3} (solid line) and 5×10^{-4} A cm^{-3} (dotted line).

distribution, Fig. 14, is almost unchanged while there is a relatively large effect on the polarization behaviour, Fig. 15. The cell voltage during discharge can thus be improved by increasing the active surface area. It is also possible to increase the apparent exchange current density of the lead dioxide electrode by decreasing the acid concentration. In that case, the effects must be compared with changes in discharge capacity due to more rapid acid depletion during discharge. However, changing the kinetic parameters is not an alternative for improving the current distribution in the cell.

It has been shown that the model can be used to predict the polarization behaviour and the initial local rate of discharge of the active material in both the negative and the positive electrodes of lead–acid cells with tubular lead dioxide electrodes. It has also been shown that the separator has a minor effect on the potential and current density distribution, while the tube envelope influences the discharge behaviour to a large extent. This is in accordance with earlier results obtained with the one-dimensional discharge model [10, 11]. The two-dimensional analysis of the current density distribution shows that there can be large variations in the rate of discharge in different parts of the positive electrode and that it to a large extent depends on the properties of the tube envelope. The presence of an envelope makes the current distribution around the outer parts of the electrode tube more uniform and the envelope acts as a current leveller due to its additional and relatively high effective resistivity. The limit of this effect would be when the current is uniformly distributed over the electrode tube. It would then be equal to the one-dimensional case studied in [10] and [11]. This means that it is more accurate to regard the cell as one-dimensional if the positive tubes have envelopes compared with tubes without envelope. The assumptions previously made can therefore be understood and to some extent justified. In addition, it has also been experimentally shown [10] that the effect of cell geometry on discharge capacity is very small compared with the effects of the envelope. It is also reasonable to assume that any nonuniform current loads on the outer surface of the electrode tube would tend to counterbalance themselves by formation of more lead sulphate that subsequently will give a more uniform utilization around the electrode.

This discussion, together with the model output, is in contradiction to the results presented by Lin, Wang and Wan [9], who stated that the inner parts of a tubular lead dioxide electrode are discharged before the outer parts. This fact has also been discussed earlier in [10] and [11].

The results from the work on an electrical analogue circuit as a model for the tubular lead dioxide electrode, presented by Euler and Horn [12], showed that the initial current density distribution would be fairly uniform. Their measurements indicated a maximum deviation from the mean local current density of 2.1%. They also stated that the potential drop along the height of the cell is much more significant and could result in deviations from the mean current density of about 10%. From what has been found in this investigation, it can be stated that the current density distribution over the cross section of the electrode tubes is more nonuniform than what Euler and Horn calculated. It has been shown that the local current densities can be about five times larger than the average local current density, sometimes even larger. This effect would therefore be larger than the effect of the vertical potential drop in the cell. However, it is probable that the tube envelope also has a positive effect on the vertical non uniformity of the current distribution. That is however beyond the scope of this paper.

7. Conclusions

The following conclusions can be extracted:

(a) The presented mathematical model can be used to analyse the initial current density and potential distribution in a lead–acid cell with tubular lead dioxide electrodes and can be used as a tool for studying the effects of different design parameters. The model was validated by experimental data.
(b) The envelope around the positive electrode has a large impact on the current density distribution and acts as a current leveller. This means that a tubular lead dioxide electrode with envelope can be treated in a one-dimensional concentric geometry with fairly good accuracy.

Acknowledgements

This work was financially supported by the Swedish National Board for Technical Development. The Royal Institute of Technology, Stockholm, is

gratefully acknowledged for the grant enabling part of this work to be made at the Texas A&M University.

References

[1] D. Simonsson, *J. Appl. Electrochem.* **3** (1973) 261.
[2] *Idem, J. Electrochem. Soc.* **120** (1973) 151.
[3] P. Ekdunge and D. Simonsson, *ibid.* **132** (1985) 2521.
[4] *Idem, ibid.* **132** (1985) 2529.
[5] *Idem, J. Appl. Electrochem.* **19** (1989) 136.
[6] *Idem, Ibid.* **19** (1989) 127.
[7] Z. Mao, R. E. White and B. Jay, *J. Electrochem. Soc.* **138** (1991) 1615.
[8] H. Gu, T. V. Nguyen and R. E. White, *ibid.* **134** (1987) 2953.
[9] K. M. Lin, Y. Y. Wang and C. C. Wan, *J. Appl. Electrochem.* **18** (1988) 590.
[10] J. Landfors and D. Simonsson, *J. Electrochem. Soc.* **139** (1992) 2760.
[11] *Idem, ibid.* **139** (1992) 2767.
[12] J. Euler and L. Horn, *Electrochem. Acta* **10** (1965) 1057.
[13] *Idem, Archiv. Electrotechnik.* **50** (1965) 85.
[14] PDE/PROTRAN, A System for the Solution of Partial Differential Equations, IMSL, Inc. (1989).
[15] G. W. Vinal, 'Storage Batteries', 4th edn, John Wiley & Sons, New York (1955).
[16] A. Lindholm, *J. Appl. Electrochem.* **13** (1983) 693.
[17] D. Berndt, 'Comprehensive Treatise of Electrochemistry', vol. 3, (edited by J. O'M. Bockris, *et al.*), Plenum Press, New York (1981).
[18] A. Lindholm, *J. Appl. Electrochem.* **10** (1983) 7.
[19] H. Bode, 'Lead-Acid Batteries', 4th edn, Wiley-Interscience, New York (1977).
[20] L. von Rudolf, *Elektrotechn. Z.* **86** (1965) 431.
[21] 'Handbook of Chemistry and Physics', 65th edn (edited by R. C. Weast), CRC Press, Boca Raton, FL (1985).
[22] O. E. Abdel-Alam, *J. Power Sources* **30** (1990) 227.
[23] A. Lindholm, *J. Power Sources* **10** (1983) 71.
[24] J. Newman and W. Tiedemann, *AIChE J.* **21** (1975) 25.